Remote optical detection using microcantilevers

E. A. Wachter,[a] T. Thundat, P. I. Oden, and R. J. Warmack
Health Sciences Research Division, Oak Ridge National Laboratory, Oak Ridge, Tennessee 37831

P. G. Datskos and S. L. Sharp
Consultec Scientific, Inc., Knoxville, Tennessee 37932

(Received 20 February 1996; accepted for publication 29 July 1996)

The feasibility of microcantilever-based optical detection is demonstrated. Microcantilevers may provide a simple means for developing single-element and multielement infrared sensors that are smaller, more sensitive, and lower in cost than quantum well, thermoelectric, or bolometric sensors. Here we specifically report here on an evaluation of laboratory prototypes that are based on commercially available microcantilevers, such as those used in atomic force microscopy. In this work, optical transduction techniques were used to measure microcantilever response to remote sources of thermal energy. The noise equivalent power at 20 Hz for room temperature microcantilevers was found to be approximately 3.5 nW/$\sqrt{\text{Hz}}$, with a specific detectivity of 3.6×10^{7} cm $\text{Hz}^{1/2}$/W, when an uncoated microcantilever was irradiated by a low-power diode laser operating at 786 nm. Operation is shown to be possible from dc to kHz frequencies, and the effect of cantilever shape and the role of absorptive coatings are discussed. Finally, spectral response in the midinfrared is evaluated using both coated and uncoated microcantilevers. © *1996 American Institute of Physics.* [S0034-6748(96)04910-6]

I. INTRODUCTION

Infrared detection and imaging has extensive industrial, military, and commercial applications, including remote monitoring of facilities and equipment, process control, surveillance, night vision, collision avoidance, and medical imaging. Presently there are several families of commercially available infrared detectors, including thermopiles, bolometers, and various solid state detectors.[1,2] Thermopile detectors have a large thermal mass and very long response times. Bolometers using micromachined, suspended foils have much better rise times due to their reduced mass. Both thermopiles and bolometers offer broad spectral response when coated with suitable optically absorbing materials. Solid state detectors for the infrared region (such as quantum well devices) are based on semiconductor phenomena. As a consequence of their high inherent thermal noise, these devices must generally be operated at a reduced temperature; their spectral response is also limited by the intrinsic properties of the semiconductor materials.

A new approach for producing compact, light-weight, highly sensitive micromechanical infrared detectors is provided by microcantilever (MCL) technology, which functions based on the bending of a microcantilever upon absorption of optical energy. When a microcantilever is exposed to infrared radiation, the temperature of the cantilever increases due to absorption of this optical energy.[3,4] If these microcantilevers are constructed from materials exhibiting dissimilar thermal expansion properties (such as silicon nitride and thin gold film), the bimetallic effect will cause the microcantilever to bend in response to this temperature variation.[3–10] This response is shown in Fig. 1. The extent of bending is directly proportional, in first order, to the rate of energy absorption, which in turn is proportional to the radiation intensity. Previous work has shown that microcantilever bending can be detected with extremely high sensitivity.[11] For example, the metal-coated microcantilevers that are commonly employed in atomic force microscopy (AFM) allow sub-angstrom ($<10^{-10}$ m) sensitivity to be routinely obtained. Hence, for applications in optical radiation detection, microcantilevers can be coated with appropriate absorptive materials so that they bend upon exposure to radiation of a particular energy (such as infrared or near infrared radiation).

Standard AFM microcantilevers are typically 100–200 μm long, 0.3–3 μm thick, and 10–30 μm wide, and can be fabricated from various dielectric or semiconducting materials, such as silicon nitride. Since microcantilevers can be easily manufactured in one- and two-dimensional arrays having 500 or more individual microcantilevers on a single wafer, this technology may be practical for manufacturing sensitive infrared detector arrays with spatial resolutions comparable to current charge coupled device (CCD) detectors. In this article, we examine the interaction of microcantilevers with near infrared radiation in order to demonstrate key aspects of their behavior. The effects of microcantilever geometry and the role of absorptive coatings are also examined, along with the implications of this technology for development of new infrared imaging devices.

II. THEORY OF BIMETALLIC MICROCANTILEVER BENDING

Coated microcantilevers undergo bending due to differential stress in the cantilever. The bending, z, due to differential stress, Δs, can be written as[12]

[a]Author to whom correspondence should be addressed; Electronic mail: wachterea@ornl.gov

Downloaded¬13¬Jun¬2001¬to¬128.219.132.32.¬Redistribution¬subject¬to¬AIP¬license¬or¬copyright,¬see¬http://ojps.aip.org/rsio/rsicr.jsp

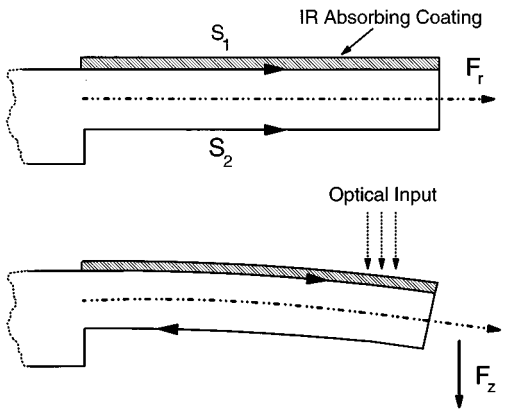

FIG. 1. Schematic diagram showing bending response of a bimetallic cantilever with an IR absorbing coating. Surface stresses S_1 and S_2 are balanced at equilibrium, generating a radial force F_r along the medial plane of the microcantilever. These stresses become unequal upon exposure to IR radiation, producing in a bending force, F_z, that displaces the tip of the microcantilever.

$$z=\frac{3l}{t_1+t_2}\left[\frac{1+\left(\frac{t_1}{t_2}\right)^2}{3\left(1+\frac{t_1}{t_2}\right)^2+\left(1+\frac{t_1}{t_2}\frac{E_1}{E_2}\right)\left(\frac{t_1^2}{t_2^2}+\frac{t_2}{t_1}\frac{E_2}{E_1}\right)}\right]\times\frac{\Delta s}{E^*}, \tag{1}$$

where t_1 and t_2 are the thickness of the coating and microcantilever substrate, l is the microcantilever length, E_1 and E_2 are the Young's moduli of the coating and microcantilever, and E^* is the effective Young's modulus of the coated microcantilever. Note that $E^*=E_1E_2/(E_1+E_2)$. Bending resulting from differential stress in such a microcantilever can be detected with subnanometer sensitivities.

Previous work has shown that silicon nitride microcantilevers with a thin gold film on one side undergo measurable bending due to temperature changes as small as 10^{-6} K. This bending is due to the differential stress created by dissimilar thermal expansion of the cantilever substrate and the gold coating (or the bimetallic effect). The differential stress due to thermal expansion of these materials can be approximated as

$$\Delta s\approx(E_1\alpha_1-E_2\alpha_2)l\Delta T, \tag{2}$$

where ΔT is the temperature change and α_1 and α_2 are the coefficients of thermal expansion for the materials composing the bimetallic strip. By measuring the bending distance z, the change in temperature can be determined by

$$\Delta T\approx\frac{E^*}{E_1\alpha_1-E_2\alpha_2}\frac{t_1+t_2}{3l^2}\times\left[\frac{3\left(1+\frac{t_1}{t_2}\right)^2+\left(1+\frac{t_1}{t_2}\frac{E_1}{E_2}\right)\left(\frac{t_1^2}{t_2^2}+\frac{t_2}{t_1}\frac{E_2}{E_1}\right)}{1+\left(\frac{t_1}{t_2}\right)^2}\right]z. \tag{3}$$

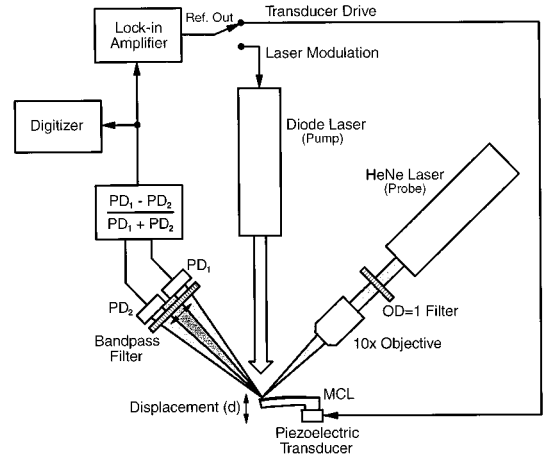

FIG. 2. Detailed schematic of the optical detection method for determining microcantilever displacement, d.

This assumes the ideal case where the cantilever and its base are at the same temperature. We have also assumed that all incident radiation is absorbed by the cantilever and the base, resulting in a uniform temperature change.

The bending of microcantilevers can be measured with high sensitivity using detection techniques commonly used in atomic force microscopy. A commercially available AFM can easily detect cantilever bending with subnanometer sensitivities, and this can be further improved by optimizing the detection system; for example Hoh *et al.*[13] and Ohnesorge *et al.*[14] have demonstrated AFM sensitivities of 10^{-11} N, corresponding to bending magnitudes of approximately 5×10^{-11} m. This implies that extremely small temperature changes can be measured using the bimetallic effect, and a 10^{-6} K temperature sensitivity should be achievable under ideal conditions.

III. EXPERIMENT

Bending of microcantilevers can readily be determined by a number of means, including optical, capacitive, and electron tunneling, and piezoresistive methods. In this article, we will concentrate on optical readout techniques for observing microcantilever bending. The approach used was adapted from standard atomic force microscopy imaging systems, and is shown in Fig. 2. Microcantilevers were mounted in a chip holder (from Digital Instruments) designed for tapping mode AFM that secured the base of the microcantilever against a small piezoelectric transducer; this chip holder was then mounted on a three-axis translation stage to facilitate fine adjustment of the microcantilever relative to the rest of the experimental apparatus. Collimated optical radiation from a diode laser was used to evenly illuminate the mounted microcantilever (pump wavelength of 786 nm, beam diameter of 6 mm, centered on the tip of cantilevers 180–320 μm in length). Output of this excitation source was modulated sinusoidally at frequencies ranging from 1 Hz to 100 kHz, with peak powers ranging from 0 to 18.5 mW (0–65 mW/cm^2). This configuration provided a flexible, easily controlled test system for quantifying microcantilever re-

Downloaded¬13¬Jun¬2001¬to¬128.219.132.32.¬Redistribution¬subject¬to¬AIP¬license¬or¬copyright,¬see¬http://ojps.aip.org/rsio/rsicr.jsp

sponse to optical energy. All measurements were conducted at ambient temperature and atmospheric conditions.

A second laser was used in a probe configuration to monitor bending. A helium–neon laser (or HeNe, delivering 3 mW at 633 nm) was focused onto the tip of the microcantilever using a 10× microscope objective; to minimize heating of the tip by the probe laser, optical power was reduced by placing a neutral density filter with an optical density of 1.0 between the probe laser and the objective. A dual-element photodiode displacement detector was used to collect the reflected probe beam (position detectors PD1 and PD2 in Fig. 2); a 1 nm band pass filter centered at 633 nm was placed in front of the detector to block scattered light from the pump laser. The difference signal from the detector pair as the cantilever tip changed position $[(PD1-PD2)/(PD1+PD2)]$ was used to measure the displacement, d. This signal was directly digitized and stored, or sent to a lock-in amplifier (SR850, Stanford Research Systems) for signal extraction and averaging. The reference output of the lock-in amplifier was also used to control modulation frequency and output level of the pump laser.

To further evaluate the optical properties of microcantilevers, a remote infrared source was used to illuminate several test microcantilevers over a band of wavelengths from 2.6 to 14 μm. Specifically, monochromatic infrared radiation from the nichrome source of a Foxboro Miran-80 infrared spectrometer was directed through atmosphere onto the surface of a microcantilever positioned approximately 30 cm from the source. Optical readout (as described above) was then used to measure microcantilever bending in response to this infrared stimulus. Since the photodiode displacement detector is blind to infrared light, no additional filtering was needed on the readout system. The Miran-80 has a 50 Hz internal chopper that provided a reference frequency for lock-in detection. Output wavelength of the Miran-80 was scanned at a rate of approximately 2.5 nm/s, and the optical bandwidth of the gradient filter used for wavelength selection was approximately 80 nm. Response of the standard detector on the Miran-80 (a lithium tantalate pyroelectric device, with a 1 s time constant) was compared with microcantilever spectra.

Optical response characteristics of three different types of commercially available AFM probe tips were evaluated. These microcantilevers are shown schematically in Fig. 3. Microcantilevers typically come from the manufacturer attached to a large rectangular chip (~1 mm wide×3 mm long×1 mm thick) that is used to facilitate manipulation and mounting, and all those evaluated in this work were used as received. The microcantilevers used were a triangular silicon nitride (Si_3N_4) microcantilever (labeled ''I'' in Fig. 3, with a length of 180 μm, a width of 18 μm, and a bending force constant $k\approx0.03$ N/m, from Park Scientific); a rectangular silicon nitride microcantilever (labeled ''II,'' 200 μm in length and 20 μm in width, bending force constant $k\approx0.02$ N/m, Park Scientific); and a triangular silicon nitride cantilever (labeled ''III,'' that was 320 μm long and 22 μm wide, with a bending force constant $k\approx0.01$ N/m, Park Scientific). Each was 0.6 μm thick. The type I cantilever was coated with aluminum on one side to see how this would affect its

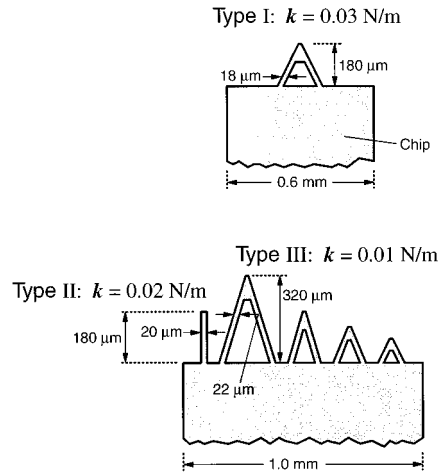

FIG. 3. Plan view of microcantilevers used for evaluation of thermal response. All were 0.6 μm thick. Note that results from only the two leftmost microcantilevers (out of five total) on the lower chip are shown.

optical response characteristics; types II and III were used as received from the manufacturer, with a gold/chromium film uniformly covering one side. Additionally, another set of type III microcantilevers were used to measure infrared spectral response. This set consisted of a reference cantilever and test cantilever, both of which were coated with the original manufacturer's gold/chromium film. The test cantilever was further coated on the surface opposite the metal film with a thin layer of the laser dye HITC (1,1′,3,3,3′,3′-hexamethylindotricarbocyanine iodide, CAS No. 19764-96-6).

IV. RESULTS AND DISCUSSION

An essential aspect of any scheme for micromechanical optical detection is the ability to sensitively detect physical changes resulting from thermal stress, since this directly affects the sensitivity and precision in measurement of temperature change or thermal flux. As an initial evaluation of the ability to detect optically induced bending of a microcantilever, each of the three types of microcantilever were subjected to both mechanical and optical excitation, and their response measured as a function of excitation frequency. Mechanical excitation was achieved by driving the piezoelectric element in the AFM chip holder with the reference signal from the lock-in amplifier; such mechanical excitation spectra are helpful in locating resonance frequencies for allowed microcantilever bending modes. Optical excitation spectra were obtained by modulating the pump laser with the lock-in reference signal. Typical response spectra for a triangular microcantilever (type III) are shown in Fig. 4. The mechanical spectrum (curve ''A'') shows two resonances, at 6 and 38 kHz, attributable to the fundamental transverse resonance and a higher-order resonance (possibly torsional bending), respectively. The optical spectrum (curve ''B'') shows similar resonance features, although with somewhat different relative intensities; a large, broadband response is also noted at low frequencies. No synchronous oscillatory response was noted when the microcantilever was excited

Downloaded¬13¬Jun¬2001¬to¬128.219.132.32.¬Redistribution¬subject¬to¬AIP¬license¬or¬copyright,¬see¬http://ojps.aip.org/rsio/rsicr.jsp

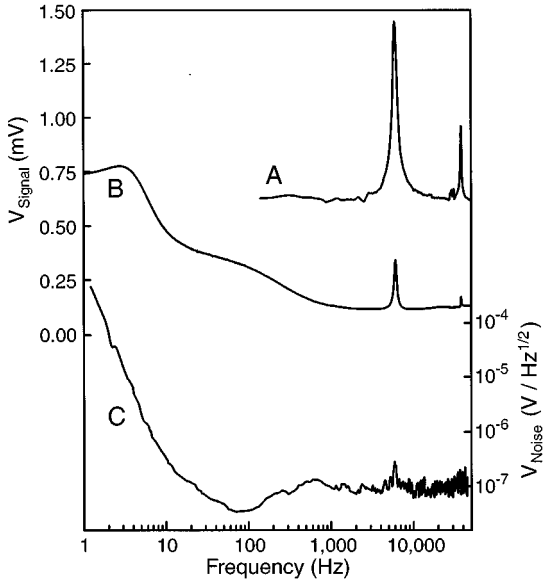

FIG. 4. Mechanical and optical excitation spectra for a type III microcantilever. Response to frequency swept mechanical excitation is given in spectrum (A): similar results for optical excitation are shown in spectrum (B). Optical excitation was effected using a sinusoidally modulated pump laser at 786 nm. Spectrum (C) shows noise response with the pump laser operated in a dc mode. Fundamental mechanical resonance at 6 kHz and higher-order resonance at 38 kHz are evident for both optical and mechanical excitation.

with constant dc laser power (curve ''C''). A similar response was noted under these conditions for the other two microcantilevers.

Figure 4(B) shows that microcantilever response to optical input decreases rapidly for frequencies above 10 Hz but that mechanical resonance is still observed even at frequencies well above 10 kHz. In fact, the type I and II microcantilevers (Fig. 3) exhibited strong optical resonance at frequencies of 17 and 14 kHz, respectively; these modes correspond to the fundamental transverse resonances for the microcantilevers. Such resonant response demonstrates that reversible heating and bending of the cantilever occurs as a result of optical excitation, producing mechanical vibration. These resonances also have quality factors that are identical to their mechanically driven counterparts, confirming that optically pumped mechanical vibration is occurring.

The rapid rolloff in response observed in Fig. 4(B) is likely to be due to thermal equilibration of the cantilever at high modulation frequencies. Because the cantilever must dissipate heat between laser cycles, the finite thermal conductivity of its legs limits the rate at which heat from these thermal impulses can be transferred out of the microcantilever and into the support structure (the chip); thus, as modulation frequency is increased and the microcantilever approaches thermal equilibrium, changes in thermal stress as a function of time approach zero. Comparison of the response of the type II and type III cantilevers showed that the rectangular type II microcantilever had a higher relative response at frequencies above 7.5 kHz. We believe this is due to more effective thermal transfer for the rectangular geometry. Since the rectangular microcantilever does not have a geometric restriction between the cantilever and the chip, transfer of thermal energy absorbed at the tip should be more rapid than

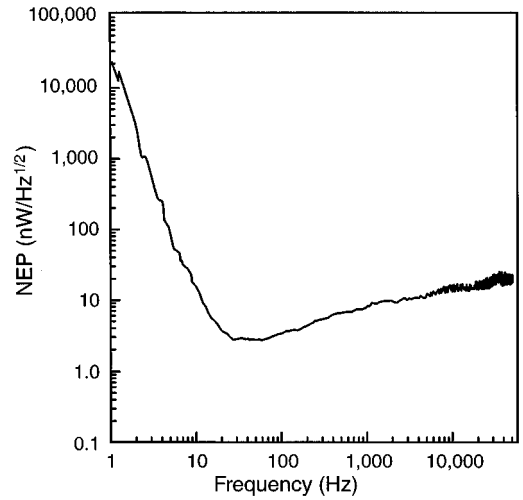

FIG. 5. Noise equivalent power (NEP) as a function of modulation frequency for a type III silicon nitride microcantilever. Optical excitation at 785 nm, utilizing bimetallic bending induced in a gold/chromium film.

that for the triangular microcantilever, which has a large area tip suspended on relatively narrow legs. The direct route of thermal transfer in the rectangular microcantilever appears to allow it to maintain a thermal differential at higher optical modulation frequencies, and hence to continue responding to the time varying optical stimulus at frequencies well above those practical with the triangular geometry.

To evaluate the role of optical reflectivity (or thermal absorptivity) on microcantilever response, a silicon nitride microcantilever (the type I specimen) was coated on one side with a thin layer of aluminum; we should note that the manufacturer's gold/chromium film was removed prior to aluminum deposition. This produced a microcantilever that had a nearly transparent body that was highly reflective to the pump laser on the aluminum coated side (reflectivity, $R \approx 0.95$ at 786 nm), but slightly less reflective on the uncoated side (due to absorption of the pump radiation upon

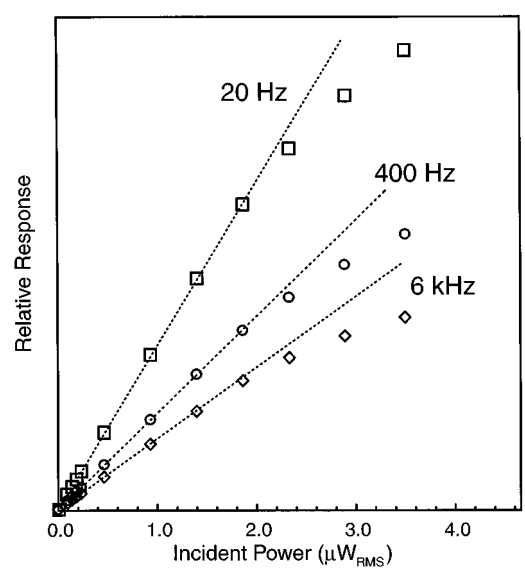

FIG. 6. Photometric response for a typical microcantilever (type III) at various optical pump levels, using excitation at 20 Hz, 400 Hz, and 6 kHz.

Downloaded¬13¬Jun¬2001¬to¬128.219.132.32.¬Redistribution¬subject¬to¬AIP¬license¬or¬copyright,¬see¬http://ojps.aip.org/rsio/rsicr.jsp

TABLE I. Photometric response at 785 nm for a gold/chromium coated Si_3N_4 microcantilever (type III). Data at 6.02 kHz obtained at mechanical resonance for the microcantilever.

Optical modulation frequency (Hz)	Detector time constant (ms)	V_{signal} (μV)	V_{noise} (μV)	NEP (nw/$\sqrt{}$Hz)	D^* (cm Hz$^{1/2}$/W)
6020	300	307.1	0.585	13.1	9.48×10^6
	30	305.3	1.76	12.5	9.91×10^6
	1	305.5	9.46	12.3	1.01×10^7
400	300	223.2	0.196	6.03	2.06×10^7
	30	221.1	0.691	6.78	1.83×10^7
	10	226.3	1.19	6.59	1.88×10^7
20	300	528.2	0.266	3.46	3.59×10^7

transmission through the Si_3N_4 cantilever body). As expected, the resonant frequency of this cantilever was found to be 17 kHz. However, when the uncoated side of the microcantilever was illuminated (reverse geometry), the magnitude of bending response at all frequencies increased by about 20% in comparison to normal illumination on the reflective side. We believe this difference is attributable to increased absorption of the pump beam upon transmission through the Si_3N_4 material, resulting in more effective transduction of optical energy into thermal heating of the microcantilever. While this simple experiment demonstrate that sensitivity can be improved by increasing absorption of impinging optical radiation, it is obvious that appropriate optically absorbing coatings are needed to fully optimize the method (such as carbon black, gold black, or other broadband absorbers). Unfortunately, such materials were not available for this study.

Photometric response was further characterized by measuring microcantilever response at various modulation frequencies and optical pump levels (Figs. 5 and 6, and Table I). For the type III Si_3N_4 microcantilever, we estimate a noise equivalent power (NEP) of 3.5 nW/$\sqrt{}$Hz at 20 Hz, where $\mathrm{NEP}=(V_{noise}/\sqrt{B})(P/V_{signal})$, V_{noise} is the background noise level on the cantilever over a lock-in amplifier bandwidth, B, of 0.26 Hz, and P is the incident optical power producing an observed signal, V_{signal}. Specific detectivity, D^*, is equal to 3.6×10^7 cm Hz$^{1/2}$/W under these conditions, where $D^*=(A^{1/2}/V_{signal})/(V_{noise}/P)$, and A is the area of the detector element. Note that the characteristics of this initial, unoptimized microcantilever compare quite favorably with some room temperature technologies currently under development, including indium antimonide photoconductors (NEP=40 nW at 250 Hz),[15] but are not yet competitive with silicon microbolometers [NEP=5 pW/$\sqrt{}$Hz, noise equivalent temperature difference (NETD)=40 mK at 30 Hz][16] or pyroelectric devices (NEP=8 pW/$\sqrt{}$Hz, $D^*=3.5\times10^8$ cm Hz$^{1/2}$/W).[17] However, in contrast to these highly optimized examples, several simple improvements to our microcantilever system are obvious that could improve performance dramatically. For instance, since the metal coating on the tested cantilevers is highly reflective at the pump wavelength (for gold, $R>98\%$ at 785 nm), use of an improved absorptive coating (such as gold black, $R<2\%$) could improve NEP in this example to <75 pW. Furthermore, the observed detection limits appear to be determined by readout noise in our optical detection circuit. We believe that, with careful design of this circuitry, performance could be substantially improved. Finally, response of the microcantilevers was extremely linear (with a correlation coefficients, $r^2>0.999\,95$) except at very high laser modulation test levels; this rolloff in measured response at high modulation levels is an artifact of our method for modulating the pump laser, which exhibited a reduced depth of modulation at high drive levels.

Spectral response of silicon nitride microcantilevers was evaluated at infrared wavelengths ranging from approximately 2.6 to 14 μm using a tunable infrared source. Example performance is shown in Fig. 7, which shows optically stimulated response for microcantilevers over a band from 6.0 to 7.8 μm. Of note is the fact that the gold/chromium coated silicon nitride microcantilever (curve A) displayed similar spectral response to that of a commercial lithium tantalate pyroelectric detector (curve C). The common feature between 6.0 and 6.6 μm in curves A and C appears to be due to atmospheric absorbance attributable to water vapor. Over

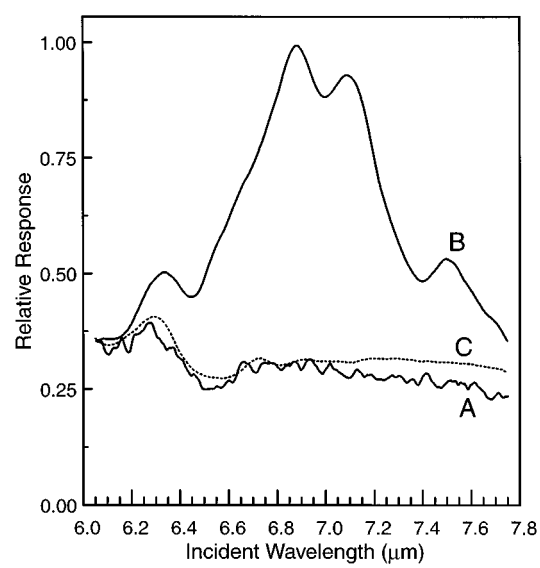

FIG. 7. Infrared spectral response of silicon nitride microcantilevers and of a commercial lithium tantalate pyroelectric detector. Response for a gold/chromium coated silicon nitride microcantilever (curve A) and a similar microcantilever coated with a thin film of the laser dye HITC (curve B) are compared to that for the pyroelectric device (curve C). Curve C has been normalized to show a relationship to curve A.

Downloaded¬13¬Jun¬2001¬to¬128.219.132.32.¬Redistribution¬subject¬to¬AIP¬license¬or¬copyright,¬see¬http://ojps.aip.org/rsio/rsicr.jsp

the 30 cm optical path between the source and detectors, such a band is to be expected. When a similar microcantilever to that used to obtain curve A was coated with an organic dye molecule (HITC) the spectral response changed dramatically (curve B). The increase in response throughout this band is indicative of increased absorption of incident light by the HITC coating. These features are consistent with expected infrared absorption bands for HITC attributable to aliphatic C–H bending at 6.8 μm and aromatic C═C stretching at 6.3 μm. Furthermore, comparison of the magnitude of microcantilever response in curves A and B clearly indicates that vastly increased photometric sensitivity can be achieved if suitable absorptive coatings are used.

V. DISCUSSION

The results of this study demonstrate that microcantilevers represent an important development in room temperature infrared detector technology, and can be expected to provide the basis for considerable further development. For example, while the microcantilevers employed here were optimized for standard AFM applications (and were in fact designed to minimize thermal sensitivity), vastly improved detectors could be produced by making relatively simple changes in the materials and geometries used in microcantilever fabrication. It is possible to design microcantilevers with much smaller force constants by varying the geometry of the cantilever, and in contrast to the devices used in this study, cantilevers with force constants as small as 0.008 N/m are now commercially available. Since the fundamental mechanical resonance frequency of a microcantilever is proportional to $k^{1/2}$, reductions in force constant can be used to bring resonance into ranges compatible with mechanical chopping frequencies. It is also clear that the coatings applied to the cantilever are at least as important as the composition of the cantilever itself. For example, high thermal expansion bimetallic coatings (such as films of Al, Zn, Pb, or In) could be used to increase the thermally induced bending of the cantilever. Coating the surface of the cantilever with high emissivity materials (such as gold black) should also enhance infrared response.

Since microcantilever spectral response can be easily tailored through the application of specific absorptive coatings, choice of material for fabrication of the microcantilever can be determined primarily by the requirements of the manufacturing process. This means that microcantilevers can be fabricated using standard semiconductor methods and materials, and as a consequence could be mass produced at very low cost. Hence, two-dimensional cantilever arrays based on the technology described here could become very competitive with existing technologies due to their inherent simplicity, high sensitivity, and rapid response to optical radiation. While the optical readout method employed in this study is useful with single element designs, practical implementation of microcantilever arrays may require the use of other readout methods, such as piezoresistance. Fortunately, the microcantilever technology's compatibility with a variety of readout methods also affords tremendous flexibility to potential system designers.

ACKNOWLEDGMENTS

Research was sponsored by the U.S. Department of Energy under Contract No. DE-AC05-96OR22464 with Lockheed Martin Energy Research Corp. The authors wish to acknowledge the support of the ORNL Seed Money Program. The efforts of P.I.O. were supported in part by an appointment to the Alexander Hollaender Distinguished Postdoctoral Fellowship Program sponsored by the U.S. Department of Energy, Office of Health and Environmental Research, and administered by the Oak Ridge Institute for Science and Education. Two authors (P.G.D. and S.L.S.) wish to acknowledge the support of the National Science Foundation under SBIR Award No. DM2-9460929 to Consultec Scientific, Inc.

[1] *Optical and Infrared Detectors*, Vol. 19 of Topics in Applied Physics, edited by R. J. Kayes (Springer, Berlin, 1977).
[2] P. Howard, J. Stevens, C. Rau, R. J. Herring, and R. A. Wood, *Infrared Technology XXI* (SPIE Bellingham, WA, 1995), Vol. 2552, p. 60.
[3] J. R. Barnes, R. J. Stephenson, C. N. Woodburn, M. E. Welland, T. Rayment, J. K. Gimzewski, and Ch. Gerber, Rev. Sci. Instrum. **65**, 3793 (1994).
[4] O. Nakabeppu, M. Chandrachood, Y. Wu, J. Lia, and A. Majumdar, Appl. Phys. Lett. **66**, 694 (1995).
[5] N. Umeda, S. Ishizaki, and H. Uwai, J. Vac. Sci. Technol. B **9**, 1318 (1991).
[6] M. Allegrini, C. Astoli, P. Baschieri, F. Dinneli, C. Frediani, A. Lio, and T. Mariani, Ultramicroscopy **42–44**, 371 (1992).
[7] O. Marti, A. Ruf, M. Hipp, B. Bielefeldt, J. Colchero, and J. Mlynek, Ultramicroscopy **42–44**, 345 (1992).
[8] J. Mertz, O. Marti, and J. Mylnek, Appl. Phys. Lett. **62**, 2344 (1993).
[9] J. K. Gimzewski, Ch. Gerber, E. Meyer, and R. R. Schlitter, Chem. Phys. Lett. **217**, 589 (1994).
[10] T. Thundat, R. J. Warmack, G. Y. Chen, and D. P. Allison, Appl. Phys. Lett. **64**, 2894 (1994).
[11] D. Sarid, *Scanning Force Microscopy* (Oxford University Press, New York, 1991).
[12] P. J. Shaver, Rev. Sci. Instrum. **40**, 901 (1969).
[13] J. H. Hoh, J. P. Cleveland, C. B. Prater, J. P. Revel, and P. K. Hansma, J. Am. Chem. Soc. **114**, 4917 (1992).
[14] F. Ohnesorge and G. Binnig, Science **260**, 1451 (1993).
[15] R. Anton, E. L. Dereniak, and J. Garcia, in Ref. 2, p. 592.
[16] N. Butler, R. Blackwell, R. Murphy, R. Silva, and C. Marshall, in Ref. 2, p. 583.
[17] S. Fujii, T. Kamada, S. Hayashi, Y. Tomita, R. Takayama, T. Hirao, T. Nakayama, and T. Deguchi, in Ref. 2, p. 612.

Downloaded¬13¬Jun¬2001¬to¬128.219.132.32.¬Redistribution¬subject¬to¬AIP¬license¬or¬copyright,¬see¬http://ojps.aip.org/rsio/rsicr.jsp